Journal of Materials Chemistry C

ROYAL SOCIETY OF CHEMISTRY

PAPER

View Article Online
View Journal | View Issue

Cite this: J. Mater. Chem. C, 2023, 11, 8154

Impact of two diammonium cations on the structure and photophysics of layered Sn-based perovskites†

Eelco K. Tekelenburg, Nawal Aledlbi, Lijun Chen, Graeme R. Blake and Maria A. Loi *

Received 31st October 2022,
Accepted 4th January 2023

DOI: 10.1039/d2tc04626a

rsc.li/materials-c

Layered metal-halide perovskites have shown great promise for applications in optoelectronic devices, where a large number of suitable organic cations give the opportunity to tune their structural and optical properties. However, especially for Sn-based perovskites, a detailed understanding of the impact of the cation on the crystalline structure is still missing. By employing two cations, 2,2′-oxybis(ethylammonium) (OBE) and 2,2′-(ethylenedioxy)bis(ethylammonium) (EDBE), we obtain a planar ⟨100⟩ and a corrugated ⟨110⟩-oriented perovskite, respectively, where the hydrogen bonding between the EDBE cations stabilises the corrugated structure. $OBESnI_4$ exhibits a relatively narrow band gap and photoluminescence bands compared to $EDBESnI_4$. In-depth analysis shows that the markedly different optical properties of the two compounds have an extrinsic origin. Interestingly, thin films of $OBESnI_4$ can be obtained both in black and red colours. This effect is attributed to a second crystalline phase that can be obtained by processing the thin films at 100 °C. Our work highlights that the design of the crystal structure as obtained by ligand chemistry can be used to obtain the desired optical properties, whereas thin film engineering can result in multiple crystalline phases unique to Sn-based perovskites.

10th Anniversary Statement written by Maria A. Loi

I was a young post-doctoral fellow when, at that time Journal Material Chemistry, published my work on the photophysics and solar cells of phthalocyanine–fulleropyrrolidine dyads and devoted the cover to the article. From that moment, I have been always considering the Journal Material Chemistry family, and especially Journal Material Chemistry C, as the perfect avenue for multidisciplinary works where new materials, deep spectroscopical investigation and even device investigations can be presented to a multifaceted community. The interdisciplinarity, breadth and plasticity in embracing the newest topics emerging from the community are the characteristics, that in my opinion, determine the continuous success of Journal Material Chemistry C. Now Journal Material Chemistry C is 10 years old but does not give any signs of ageing or rigidity. As modern science is highly accelerated, this is a merit of the team running the journal. Happy birthday to Journal Material Chemistry C, wishing it many years of youth ahead.

Introduction

Layered metal-halide perovskites are at the forefront of emerging light-emitting materials and already have proven their invaluable contributions to photovoltaic devices and light-emitting diodes.[1–3] This class of materials offers a vast amount of different crystal structures due to its flexibility to accommodate a large number of organic cations.[2,4] Of the large organic cations used, most reports focus on monoammonium cations such as butylammonium and phenethylammonium. Recently, diammonium cations are gaining momentum because of the hope to obtain different functionalities, and the power conversion efficiency of solar cells is increasing using diammonium cations.[5] These structures show exotic phenomena, enabling the design of materials that emit either narrow or broad photoluminescence (PL) bands.[6,7]

The origin of the optical properties of layered perovskites lies in the connectivity of the inorganic framework, where we can distinguish two main types: the ⟨100⟩- and the ⟨110⟩-oriented perovskites.[8,9] These structures can be envisioned as slices of the cubic perovskite structure along the ⟨100⟩ or the ⟨110⟩ crystallographic planes and are separated by organic cations. For this reason, the ⟨100⟩-type consists of flat layers of corner-shared inorganic octahedra with metal-halide-metal

Zernike Institute for Advanced Materials, University of Groningen, Nijenborgh 4, 9747 AG, Groningen, The Netherlands. E-mail: m.a.loi@rug.nl

† Electronic supplementary information (ESI) available: Experimental details, further experimental data, photoluminescence spectroscopy, structural parameters. CCDC 2204974 and 2204975. For ESI and crystallographic data in CIF or other electronic format see DOI: https://doi.org/10.1039/d2tc04626a

angles close to 180°, while the ⟨110⟩-type consists of corrugated sheets with angles close to 90° among inorganic octahedra. Interestingly, the vast majority of layered metal halide perovskites adopt the ⟨100⟩-type structure, and it remains challenging to predict which cations can favour ⟨110⟩-type structures.[10] However, from empirical studies, it is clear that cation size and intercation interactions (through halide or hydrogen bonding) are important factors that stabilise the ⟨110⟩-type.[9–11]

Owing to the pioneering work by Dohner *et al.*, the optical properties of a number of ⟨110⟩ perovskites were investigated, of which some compounds employed 2,2′-(ethylenedioxy)bis(ethylammonium) (EDBE).[11,12] It was shown that the band gap of ⟨110⟩ perovskites is typically wider than the ⟨100⟩ counterpart, where some of the ⟨110⟩ perovskites showed broad emission bands attributed to the emission from self-trapped excitons. These works inspired further exploration and a number of other ⟨110⟩ perovskites have been reported since.[2,13,14] It is not known if the length of the EDBE cation is important to stabilise this structure. In addition, a survey through the ⟨110⟩ perovskites shows that most of the compounds contain Pb, whereas very little has been done with the environmentally more benign Sn. In particular, much is unknown about the optical properties of these Sn-based perovskites and remains to be explored.

Layered Sn-based perovskites have shown intriguing structural flexibility where the same organic cations result in two distinct crystalline structures.[15–17] For example, Mao *et al.* found that the kinetic product of the synthesis in hydroiodic acid formed red crystals of the ⟨110⟩ type, while the thermodynamically stable black crystals crystallised in the ⟨100⟩ type.[15] However, thus far, only structural isomers were found for single crystals, yet applying them in thin films could open new pathways to tune the optoelectronic properties of these materials in device applications.

In this report, we address the need to comprehend the structure and optical properties of layered Sn-based perovskites, where we systematically investigate two diammonium organic cations that vary in length: 2,2′-oxybis(ethylammonium) (OBE) and 2,2′-(methylenedioxy)bis(ethylammonium) (EDBE). A marked contrast is obtained as $OBESnI_4$ forms a ⟨100⟩-oriented perovskite with relatively narrow emission peaks compared to the broad emission obtained with the ⟨110⟩-oriented $EDBESnI_4$. We show through temperature and power-dependent photoluminescence measurements that the low-energy emission in these compounds is extrinsic in nature. These compositions were successfully fabricated into thin films by a blade-coating deposition process. Furthermore, we reveal that the annealing temperature of the thin films of $OBESnI_4$ drastically changes the colour of the films from black to red. This change in colour originates from a new crystalline phase marking the structural and optical flexibility of layered Sn-based perovskites.

Results and discussion

We synthesised mm-sized single crystals of $OBESnI_4$ and $EDBESnI_4$ using an Anti-Solvent Vapour Crystallisation method, see ESI† for the details. A striking colour difference is seen for the two crystals: black-brown for $OBESnI_4$ and orange-red for $EDBESnI_4$, as shown in Fig. 1(a and b). We used X-ray diffraction (XRD) to unravel their crystal structures, which are depicted in Fig. 1(c and d) for $OBESnI_4$ and $EDBESnI_4$, respectively. Both structures were solved in the $P2_1/c$ space group (structural parameters are shown in Table S1, ESI†), although two types of structures were formed. $OBESnI_4$ consists of planar inorganic sheets separated by the diammonium cation, forming a ⟨100⟩-type layered structure. In contrast, $EDBESnI_4$ forms corrugated sheets of the ⟨110⟩ type, where the inorganic octahedra are linked to each other with angles close to 90°. It is remarkable that a small difference in the cation length can induce such large differences in the structure. A further examination of the structure revealed that hydrogen bonds are formed between EDBE cations, see the inset of Fig. 1(d), which are absent in $OBESnI_4$. Hence, the additional length of the EDBE cation is of key importance to form these hydrogen bonds, which subsequently stabilise the corrugated structure.[12]

To further investigate the impact of the structure on the optical properties, we measured the Kubelka–Munk transformed diffuse reflectance F(R) and PL spectra of the two compounds at room temperature (Fig. 1(e and f)). In line with the colour difference, $EDBESnI_4$ shows an absorption peak at 2.36 eV, a much higher value than the 1.99 eV for $OBESnI_4$. This large difference can be readily understood by considering the octahedral connectivity and the band edge orbitals of the compounds. Due to the antibonding character of both the valence (Sn 5s and I 5p) and conduction (Sn 5p and I 5p) band edge, the Sn–I–Sn angle has a major impact on the electronic and optical band gap.[18] The close to 90° angles between octahedra in $EDBESnI_4$ decrease the orbital overlap, resulting in a widening of the band gap compared to $OBESnI_4$.[16]

The PL spectra of the two compounds exhibit different features. The PL of $OBESnI_4$ shows two peaks at 1.90 eV and 1.96 eV relatively close to the absorption edge. The relative intensity of the two peaks varies across the samples (Fig. S1(a), ESI†), and the high-energy peak becomes the dominant emission at high excitation fluences as the low-energy emission saturates (Fig. S1(b), ESI†), which suggests that the low-energy emission has an extrinsic origin, *i.e.* emission from defects. The PL of $EDBESnI_4$ shows a broad emission band at 1.61 eV with a Stokes shift of ≈700 meV, the first report on such a Sn-based system. Interestingly, the related Pb-based $EDBEPbI_4$ shows a much narrower emission that shows features closely resembling $OBESnI_4$,[11,19] while broad emissions are more commonly observed for bromide and chloride containing systems.[20] To test the stability of our compounds, we measured the PL spectra by continuously illuminating the samples with our laser for 10 minutes in a nitrogen environment, as shown in Fig. S7 (ESI†). Only minor fluctuations in intensity are observed, indicating that our Sn-based layered structures show good stability.

To further understand the optical properties of these systems, temperature-dependent PL spectra of the single crystals were measured and are shown in Fig. 2(a). We will start the discussion with $OBESnI_4$, for which three interesting observations

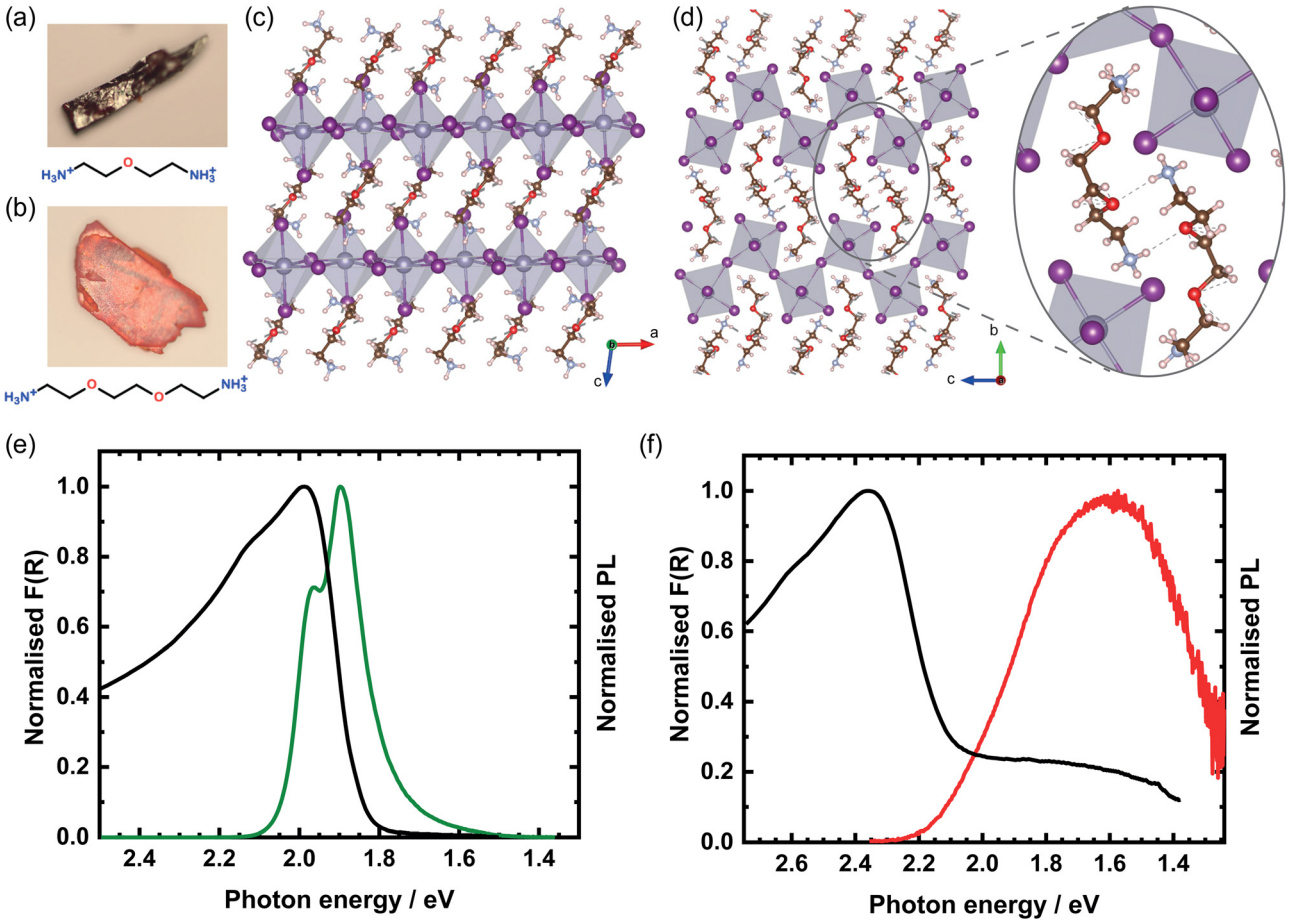

Fig. 1 (a) $OBESnI_4$ and (b) $EDBESnI_4$ images of mm-sized single crystals. Crystal structure of (c) $OBESnI_4$ and (d) $EDBESnI_4$, where grey atoms are Sn, purple are I, blue are N, brown are C, red are O, and white are H. The inset highlights the formed hydrogen bonds. Kubelka–Munk transformed diffuse reflectance and photoluminescence spectra of (e) $OBESnI_4$ and (f) $EDBESnI_4$.

can be made. (i) The emission at 1.90 eV disappears when cooling. This indicates that the low-energy emission is a thermally activated process. *Vice versa*, when the temperature is increased, the low-energy emission becomes more dominant underlining the presence of an energy barrier for this emission (Fig. S2, ESI†). A phase transition is excluded as we did not observe any appreciable change in the XRD from 100 K to 370 K. The disappearance of the low-energy peak in our diammonium compound is unique and contrasts with the appearance of a low-energy peak typically seen for monoammonium cations forming ⟨100⟩-oriented perovskites.[21,22] (ii) A blue shift is observed for the high-energy PL peak. This blue shift is unusual for metal-halide perovskites as generally the photoluminescence redshifts due to the contraction of the lattice (increasing orbital overlap) at lower temperatures. Although unusual, the overlapping tails of the absorbance and the photoluminescence in tandem with a reduced exciton-phonon coupling could cause a blue shift.[23] (iii) At 4.4 K, a substructure in the PL spectra is seen with two additional shoulders towards lower energy. Only at this low temperature, the shoulders are clearly visible as for higher temperatures the thermal energy can dissociate these bound states (see Fig. S3, ESI†). These shoulders are investigated in greater detail through fluence-dependent PL spectroscopy, as shown in Fig. 2(b). An increase of the excitation fluence over two orders of magnitude clearly shows that the relative contribution of the low-energy shoulders decreases with respect to the main peak at 2.04 eV. The approximate linear dependence of the 2.04 eV peak as a function of the excitation fluence is evidence of the free-excitonic nature of this emission, while the shoulder at 1.97 eV shows a sublinear dependence, hereby further supporting the extrinsic nature of these bound states.[24,25]

For $EDBESnI_4$, as shown in Fig. 2(a), two evident PL peaks are seen when the temperature is lowered. We note that others only observed a single broad emission band in related Pb-based systems down to 150 K.[11] The PL peaks, approximately at 1.4 eV and 1.8 eV, show a non-monotonic increase of the intensity upon decreasing the temperature (Fig. S4, ESI†), where the intensity of the peaks at 1.4 eV and 1.8 eV maximise at 30 K and 80 K, respectively. In addition, the PL lifetime of the peaks extends into the μs range at cryogenic temperatures (Fig. S5, ESI†). These observations closely resemble the intricate interplay of low-energy PL bands we reported on layered Pb-based perovskites and suggest that the main contribution to the emission stems from defects.[26] This view is supported by the sublinear dependence of the PL intensity at 4.5 K, as shown in

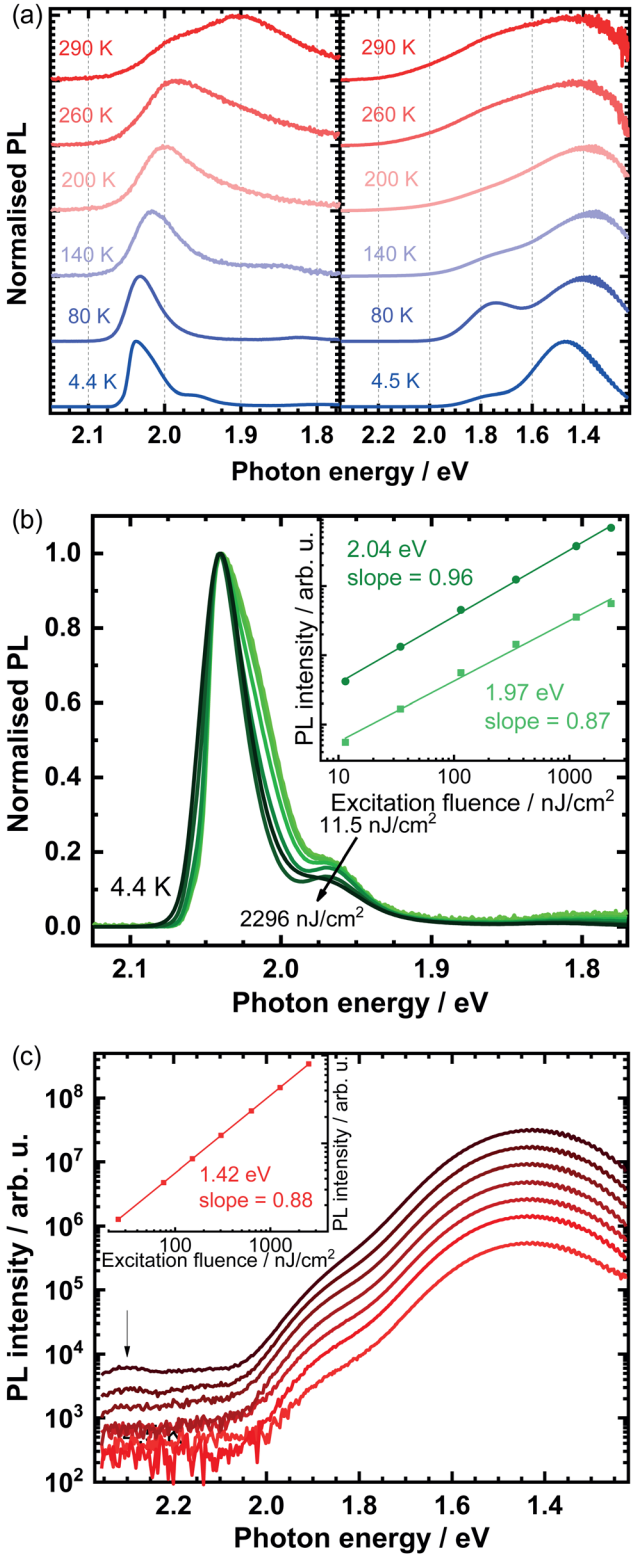

Fig. 2 (a) Temperature-dependent photoluminescence spectra of $OBESnI_4$ (left panel) and $EDBESnI_4$ (right panel). Power-dependent photoluminescence spectra at 4.4 K of (b) $OBESnI_4$ and (c) $EDBESnI_4$, where the insets show the double-logarithmic plots of the photoluminescence intensity *versus* excitation fluence.

Fig. 2(c). We note that at high fluences additional resonances are observed at approximately 2.3 eV, indicated by the arrow in Fig. 2(c).

Broad emission bands have been observed in a variety of structures, such as ⟨100⟩, ⟨110⟩, and 0D perovskites.[7,20] The origin of this emission is under intense debate and is dependent on the crystal structure as well as its elemental composition. For instance, for ⟨100⟩ and ⟨110⟩ perovskites containing bromide and chloride, the broad emission has been shown to depend on the degree of distortion of the inorganic layers and was attributed to the emission of self-trapped excitons.[11,27] In contrast, the emission from layered perovskites with iodine was ascribed to defects, where in the ⟨110⟩ perovskite $EDBEPbI_4$ colour centres were formed out of iodine interstitials.[19,26] All of these works have focused on Pb-based perovskites; it is with our work that we provide evidence that corrugated tin-iodide perovskites also have broad emission bands stemming from an extrinsic origin, *i.e.* from defects. We note that this emission is from a different origin than the broad emission in 0D tin-iodide perovskites. These 0D compounds have a high PL quantum yield owing to the emission from self-trapped excitons localised on the isolated inorganic octahedra.[28,29]

To conclude this section, we have shown that the structure of layered perovskites can be tailored by the choice of the organic cation. Critical for the stabilisation of the corrugated ⟨110⟩ structure is that EDBE can form hydrogen bonds between cations, while the smaller OBE does not form hydrogen bonds and crystallises in the ⟨100⟩-oriented perovskite. Both compounds showed photoluminescence with unusual features for Sn-based perovskites, where we discussed that the temperature plays a decisive role to observe the extrinsic nature of low-energy resonances.

Naturally, the use of $OBESnI_4$ in devices will require thin films fabricated in a scalable manner. Hence, thin films were blade coated as detailed in the ESI† and are shown in Fig. 3(a). We chose 70 °C and 100 °C as these values are typical annealing temperatures for perovskite solar cells. In addition, this allowed us to study the thin films in two cases where the crystallisation rate would change significantly. The films exhibited an unusual colour change depending on the processing temperature. For the black film, a temperature of 70 °C is used for both the doctor-blade stage and the successive annealing on a hotplate. For the red film in the middle, 100 °C is used for both processing steps. While for the film on the right, the blade coating was performed at 70 °C and the annealing on the hotplate at 100 °C. From hereon, we will refer to the films by their processing temperature for simplicity. Hence, an intriguing observation is made that the processing temperature drastically changes the optical properties of the film, where we stress that the same precursor solution was used for each of the films. To the best of our knowledge, this is the first time that such behaviour is reported in Sn-based layered perovskite thin films. We note that this temperature-dependent behaviour is exclusive to $OBESnI_4$ and is only observable during annealing when the films are still wet. Thus, heating of the fully solidified black films to 100 °C did not change the colour to red, in line with the absence of a phase transition in single crystals as discussed above.

The normalised absorbance spectra of the films are shown in Fig. 3(b). The absorbance peak of the 70 °C film at 1.98 eV matches well with the Kubelka–Munk transformed spectra

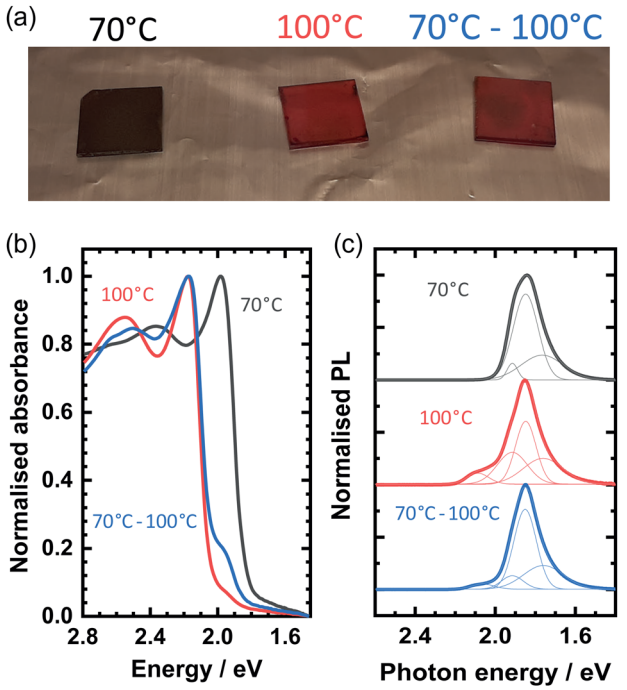

Fig. 3 (a) Optical image of $OBESnI_4$ thin films processed at 70 °C, 100 °C, and 70–100 °C. (b) Absorbance spectra and (c) photoluminescence spectra of the thin films.

shown previously in Fig. 1(e). The close correspondence of the absorbance and the measured powder X-ray diffraction patterns (Fig. S6, ESI†) to the patterns obtained from single crystals suggests that we obtained a uniform film of $OBESnI_4$ in the $P2_1/c$ phase. In contrast, the other two films have the dominant absorbance peak at 2.17 eV, where the peak at 1.98 eV manifests as a shoulder in the spectra. The presence of both of these peaks suggests that a mixture of two crystalline phases is present, where the unidentified second phase causes the appearance of the high-energy absorbance peak. Powder X-ray diffraction patterns confirm the presence of an additional crystalline phase as new reflections are observed in the 100 °C and the 70–100 °C film, which cannot be ascribed to the single crystal structure. Unfortunately, we are not able to identify the crystal structure of this phase with these data and hypothesise that a change in the octahedral connectivity or the occurrence of a corrugated structure could be the origin of this high-energy absorbance.[16,30]

This view is further supported by the photoluminescence spectra as shown in Fig. 3(c). The PL spectrum of the 70 °C film can be fitted by three Gaussian peaks centred at 1.91 eV, 1.85 eV and 1.77 eV, and shows the same spectral shape as seen for the single crystal spectrum, albeit slightly red-shifted by 50 meV. The 100 °C and the 70–100 °C film show an additional emission at approximately 2.1 eV, which matches well with an emission with a small Stokes shift from the high-energy absorbance peak. The lower intensity of the 2.1 eV PL peak could be explained by photon reabsorption of the low-energy $P2_1/c$ phase as its energy overlaps with the absorbance spectrum.

To identify the spatial extent of the two different phases, we performed confocal laser scanning microscopy on the two films as shown in Fig. 4. We investigated two spectral regions: <1.91 eV belonging to the emission from the $P2_1/c$ phase, and >1.91 eV predominantly corresponding to the unidentified phase. Fig. 4(a) shows the PL map below 1.91 eV of the 70 °C film. The film is composed of large crystallites (>100 μm), typical for doctor-blade deposition. As expected, above 1.91 eV (Fig. 4(d)), no emission is seen from a different phase. This picture drastically changes for the 100 °C (Fig. 4(b and e)) and the 70–100 °C (Fig. 4(c and f)) films. Here, the coverage of the $P2_1/c$ phase is reduced in favour of the unidentified crystal phase, where a higher processing temperature of 100 °C for the doctor-blade stage further decreases the fractional coverage of the $P2_1/c$ phase compared to a temperature of 70 °C. The images of the two spectral regions are complementary, highlighting that the two phases crystallised separately. In addition, the needle-like crystallites of the unidentified phase suggest a significant change in the unit cell compared to the $P2_1/c$ phase.

The various transitions discussed above are different from earlier observations on similar systems. Thin films based on 1,4-phenylenedimethanammonium cations showed grain-specific photoluminescence with an energy separation of 12 meV without any sign of a different crystal phase,[31] while we report a much larger 200 meV difference concomitant with the appearance of a new crystalline phase. Structural diversity in tin-iodide perovskites has been observed before in the synthesis of powders and single crystals, where structures could be stabilised by a kinetically controlled synthesis, differing from their thermodynamically stable structures.[16,32] More specifically, Mao *et al.* reported a Sn-based perovskite using histammonium that could be stabilised both in a thermodynamically stable black phase and kinetically trapped red phase.[15] This colour change originated from a change from a ⟨100⟩ to a ⟨110⟩ perovskite, where the band gap widened by 200 meV, similar to our sample. Hence, we believe that the elevated temperature of 100 °C for our thin films is sufficient to favour a structure that is in a kinetically trapped state. Considering the similar observations for OBE compared to EDBE and histammonium, we hypothesise that the kinetically formed phase might be related to a ⟨110⟩ perovskite. This observation has broader implications for the solar cell community as the processing temperature can have a drastic impact on the properties of the film and an increasing number of reports present new organic cations.

Conclusions

In conclusion, layered tin-iodide perovskite single crystals were synthesised using two different diammonium cations (OBE and EDBE), which only differ in length by two carbon and one oxygen atom. This difference has a profound impact on the structure. The shorter ODE formed a ⟨100⟩-oriented perovskite, while the larger EDBE formed a corrugated ⟨110⟩-oriented perovskite

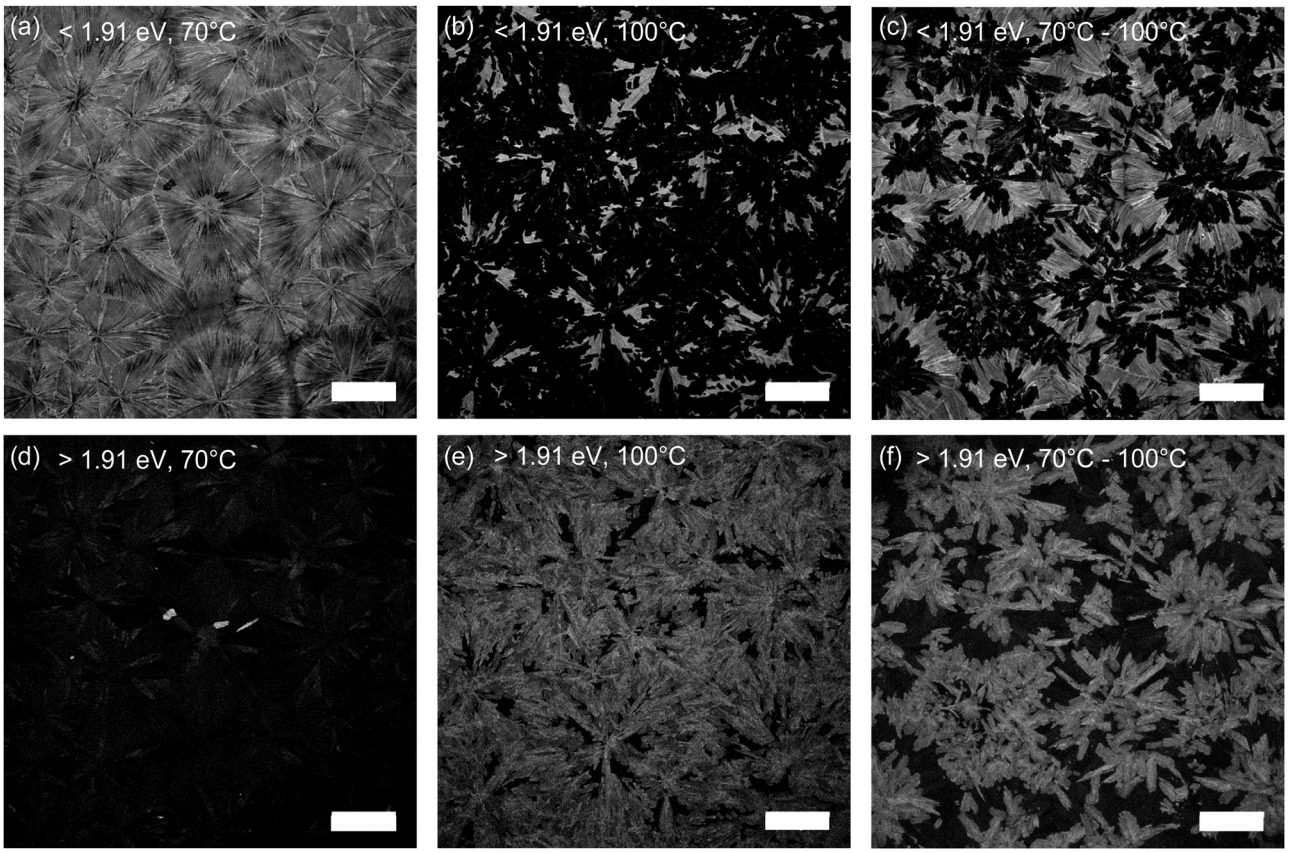

Fig. 4 Confocal photoluminescence micrographs in the range <1.91 eV (a–c) and >1.91 eV (d–f) for $OBESnI_4$ thin films processed at 70 °C, 100 °C, and 70–100 °C. Scale bar is 100 μm.

as additional hydrogen bonds were formed between neighbouring organic cations. We investigated the optical properties of the new compounds, where $OBESnI_4$ showed two photoluminescence peaks of which the low-energy emission was thermally activated. In contrast, EDBE showed a broad emission band with multiple emissive states at low temperatures, where its fluence-dependent behaviour suggests an origin from defects. Strikingly, thin films of $OBESnI_4$ showed a contrasting change of colour from black to red when the processing temperature was increased from 70 °C to 100 °C. The red colour stems from a new unidentified crystal phase that was well-separated from the black phase. With this work, we clarify how intercation interactions can result in two different types of layered perovskites with distinct optical properties, and we highlight that the processing conditions, typically used for device fabrication, have a drastic impact on the optical and structural properties of our newly reported compound.

Author contributions

E. K. T.: conceptualisation, investigation, writing – original draft N. A.: investigation, resources L. C.: resources G. R. B.: supervision, writing – review and editing, funding acquisition M. A. L. conceptualisation, supervision, writing – review and editing, funding acquisition.

Conflicts of interest

There are no conflicts to declare.

Acknowledgements

A. F. Kamp, T. Zaharia, and J. Baas are kindly acknowledged for their technical support. E. K. T. acknowledges the funding provided by the Zernike Institute of Advanced Materials – Bonus Incentive Scheme.

References

1 M. Pitaro, E. K. Tekelenburg, S. Shao and M. A. Loi, *Adv. Mater.*, 2022, **34**, 2105844.
2 X. Li, J. M. Hoffman and M. G. Kanatzidis, *Chem. Rev.*, 2021, **121**, 2230–2291.
3 A. Fakharuddin, U. Shabbir, W. Qiu, T. Iqbal, M. Sultan, P. Heremans and L. Schmidt-Mende, *Adv. Mater.*, 2019, **31**, 1807095.
4 B. Saparov and D. B. Mitzi, *Chem. Rev.*, 2016, **116**, 4558–4596.
5 S. Shao, X. Cui and Z. Li, *ACS Mater. Lett.*, 2022, **4**, 891–917.
6 C. Katan, N. Mercier and J. Even, *Chem. Rev.*, 2019, **119**, 3140–3192.

7 D. Cortecchia, J. Yin, A. Petrozza and C. Soci, *J. Mater. Chem. C*, 2019, **7**, 4956–4969.
8 D. B. Mitzi, C. A. Feild, W. T. A. Harrison and A. M. Guloy, *Nature*, 1994, **368**, 561–563.
9 D. B. Mitzi, S. Wang, C. A. Feild, C. A. Chess and A. M. Guloy, *Science*, 1995, **267**, 1473–1476.
10 Y. Y. Guo, J. A. McNulty, N. A. Mica, I. D. Samuel, A. M. Slawin, M. Bühl and P. Lightfoot, *Chem. Commun.*, 2019, **55**, 9935–9938.
11 E. R. Dohner, A. Jaffe, L. R. Bradshaw and H. I. Karunadasa, *J. Am. Chem. Soc.*, 2014, **136**, 13154–13157.
12 E. R. Dohner, E. T. Hoke and H. I. Karunadasa, *J. Am. Chem. Soc.*, 2014, **136**, 1718–1721.
13 X. Li, P. Guo, M. Kepenekian, I. Hadar, C. Katan, J. Even, C. C. Stoumpos, R. D. Schaller and M. G. Kanatzidis, *Chem. Mater.*, 2019, **31**, 3582–3590.
14 M. Ben, H. Salah, N. Mercier, M. Allain, A. Leblanc, J. Dittmer, C. Botta, C. Quarti and C. Katan, *Chem. Mater.*, 2022, **34**, 5780–5790.
15 L. Mao, H. Tsai, W. Nie, L. Ma, J. Im, C. C. Stoumpos, C. D. Malliakas, F. Hao, M. R. Wasielewski, A. D. Mohite and M. G. Kanatzidis, *Chem. Mater.*, 2016, **28**, 7781–7792.
16 C. C. Stoumpos, L. Mao, C. D. Malliakas and M. G. Kanatzidis, *Inorg. Chem.*, 2017, **56**, 56–73.
17 J. Guan, Z. Tang and A. M. Guloy, *Chem. Commun.*, 1999, 1833–1834.
18 J. L. Knutson, J. D. Martin and D. B. Mitzi, *Inorg. Chem.*, 2005, **44**, 4699–4705.
19 D. Cortecchia, S. Neutzner, A. R. S. Kandada, E. Mosconi, D. Meggiolaro, F. De Angelis, C. Soci and A. Petrozza, *J. Am. Chem. Soc.*, 2017, **139**, 39–42.
20 M. D. Smith and H. I. Karunadasa, *Acc. Chem. Res.*, 2018, **51**, 619–627.
21 G. C. Papavassiliou, I. B. Koutselas, D. J. Lagouvardos, J. Kapoutsis, A. Terzis and G. J. Papaioannou, *Mol. Cryst. Liq. Cryst. Sci. Technol., Sect. A*, 1994, **253**, 103–112.
22 G. Folpini, D. Cortecchia, A. Petrozza and A. R. Srimath Kandada, *J. Mater. Chem. C*, 2020, **8**, 10889–10896.
23 S. Wang, J. Ma, W. Li, J. Wang, H. Wang, H. Shen, J. Li, J. Wang, H. Luo and D. Li, *J. Phys. Chem. Lett.*, 2019, **10**, 2546–2553.
24 I. Pelant and J. Valenta, in *Luminescence Spectroscopy of Semiconductors*, Oxford University Press, 2012, ch. 3, pp. 82–97.
25 E. K. Tekelenburg, S. Kahmann, M. E. Kamminga, G. R. Blake and M. A. Loi, *Adv. Opt. Mater.*, 2021, **9**, 2001647.
26 S. Kahmann, E. K. Tekelenburg, H. Duim, M. E. Kamminga and M. A. Loi, *Nat. Commun.*, 2020, **11**, 2344.
27 M. D. Smith, A. Jaffe, E. R. Dohner, A. M. Lindenberg and H. I. Karunadasa, *Chem. Sci.*, 2017, **8**, 4497–4504.
28 C. Zhou, Y. Tian, Z. Yuan, H. Lin, B. Chen, R. Clark, T. Dilbeck, Y. Zhou, J. Hurley, J. Neu, T. Besara, T. Siegrist, P. Djurovich and B. Ma, *ACS Appl. Mater. Interfaces*, 2017, **9**, 44579–44583.
29 L.-J. Xu, H. Lin, S. Lee, C. Zhou, M. Worku, M. Chaaban, Q. He, A. Plaviak, X. Lin, B. Chen, M.-H. Du and B. Ma, *Chem. Mater.*, 2020, **32**, 4692–4698.
30 M. E. Kamminga, H. H. Fang, M. R. Filip, F. Giustino, J. Baas, G. R. Blake, M. A. Loi and T. T. Palstra, *Chem. Mater.*, 2016, **28**, 4554–4562.
31 S. Kahmann, H. Duim, A. J. Rommens, E. K. Tekelenburg, S. Shao and M. A. Loi, *Adv. Opt. Mater.*, 2021, **9**, 2100892.
32 C. M. Tsai, Y. P. Lin, M. K. Pola, S. Narra, E. Jokar, Y. W. Yang and E. W. G. Diau, *ACS Energy Lett.*, 2018, **3**, 2077–2085.

